Phenotype-Motivated Strategies for Optical Detection of Breast Cancer

Randall L. Barbour[1,2], Rabah Al abdi[3], Yong Xu[2], and Harry L. Graber[2]
[1]SUNY Downstate Medical Center, 450 Clarkson Ave, Brooklyn NY 11203, USA
[2]NIRx Medical Technologies LLC, 7083 Hollywood Blvd., Los Angeles CA 90028, USA
[3]Jordan University of Science and Technology, Irbid 22110, Jordan

Abstract:
Optical breast imaging studies show that controlled pressure maneuvers enhance contrast between tumors and both the surrounding healthy tissue and the contralateral breast. Our ability to detect tumors, and to distinguish them from non-cancer breast pathologies, is further improved by performing inter-breast comparisons of the reconstructed images of hemodynamic states.

Introduction:

Blood delivery to tissue, and bulk fluid redistribution among tissue compartments, frequently are impacted by disease or trauma: for example, derangements in hemodynamic states, accompanied by increased tissue stiffness and local edema, in many breast cancer cases [1]. Accordingly, we have hypothesized that dynamic responses markedly different between diseased and healthy tissues can be induced via applied-pressure or respiratory-gas maneuvers [2,3], and that diagnostic image contrast can be thereby enhanced. (See Figure 1.)

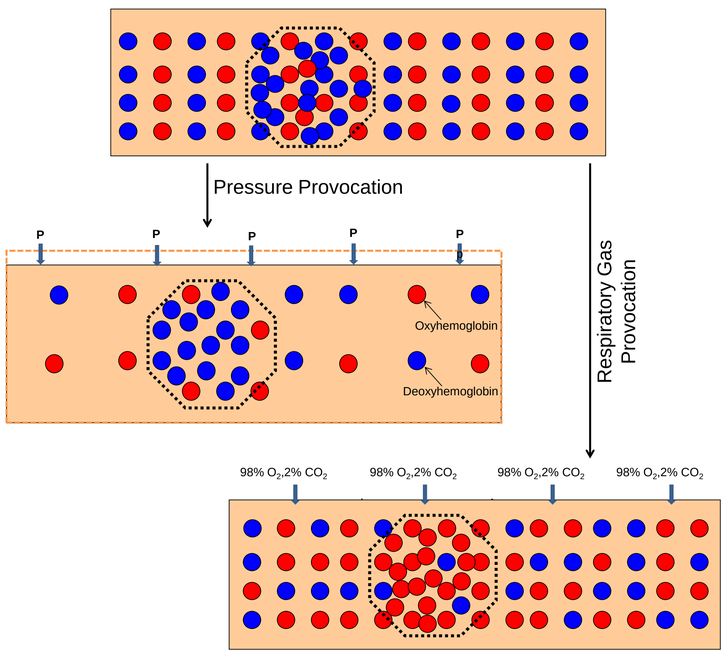

Figure 1. Tumor-biology basis for the provocations employed. Because of its increased stiffness relative to that of surrounding healthy tissue, tumor is expected to resist blood-volume redistribution in response to applied pressure. Owing to its abnormal perfusion and CO_2 response, tumor is expected to attain a higher Hb O_2 saturation in response to carbogen inspiration.

Here we present results from pilot studies conducted to evaluate the hypothesis, using an instrumentation platform that facilitates the application of the considered maneuvers, while recording time-series optical measures are obtained from both breasts simultaneously [4].

Methods:

Measurement data were obtained during an fNIRS-based breast imaging study that was conducted to evaluate the potential of applied-pressure and respiratory-gas maneuvers to enhance discovery and characterization of breast tumors (see Figure 1). After research participants gave informed consent and provided a brief medical history (for subject population demographics, see "Biomarkers for Breast Cancer Detection in the Resting-State Dynamics of the Hemoglobin Signal," this conference), they were seated and the sensing heads were adjusted to make good contact with both breasts. Following a five-minute resting baseline scan, the sequence of applied-pressure and carbogen-inspiration maneuvers depicted in Figure 2 was performed.

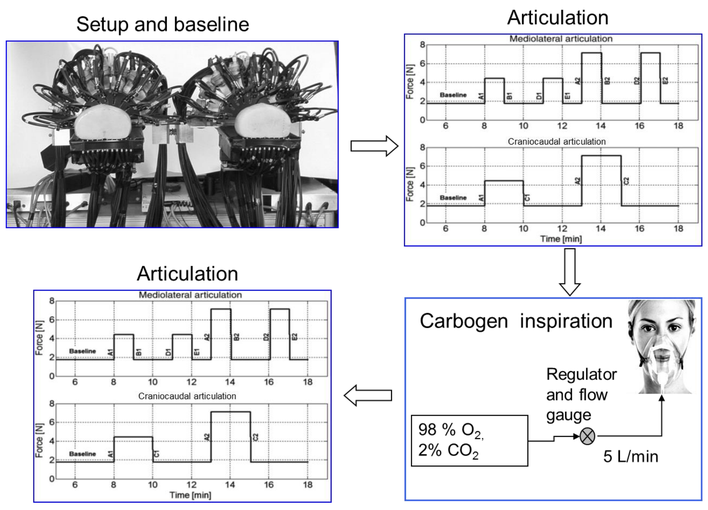

Figure 2. Schematic of the provocation time sequence applied while the fNIRS time-series recordings were performed. Optical fiber-bearing arcs seen in the upper left panel are also used for pressure application. Each arc is individually controllable, which allows for craniocaudal, mediolateral, or full compression.

The Normalized Difference Method was used to reconstruct images of absorption coefficients at the two measurement wavelengths [5].

$$\left[\frac{(u_1)_i-(u_2)_i}{(u_2)_i}\right](u_r)_i=\sum_j (W_r)_{ij}(\delta x)_j$$

u_1 and u_2 = fNIRS measurements at two different times
u_r and W_r are computed from a reference model.
δx = difference between the optical properties of the target and the reference model.

Oxygenated and deoxygenated hemoglobin (HbOxy, HbDeoxy), tissue oxygen saturation (HbSat), and blood volume (HbTot) are computed from the two-wavelength absorption coefficients.

Results:

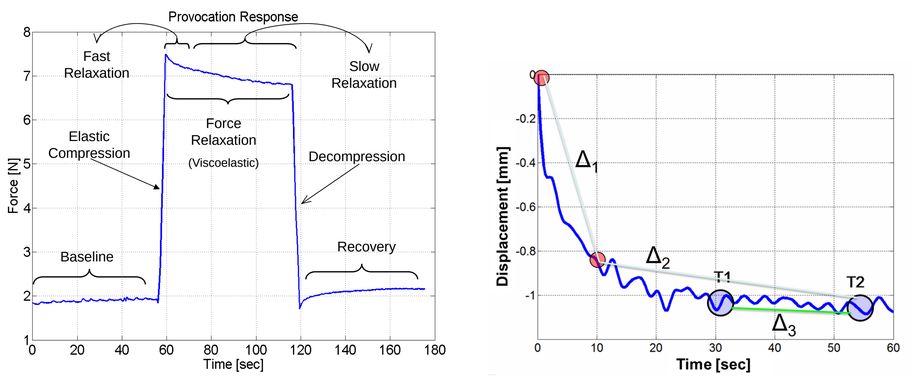

Figure 3. (Left) A representative force-vs.-time function obtained during an fNIRS recording session, with the nomenclature adopted for the different segments of the articulation maneuver indicated. (Right) An enlargement of the corresponding displacement-vs.-time function during the Force Relaxation segment. To minimize the confounding effect of optical pathlength changes, data analysis considered the hemodynamic-states changes that occurred during the Δ_3 time interval.

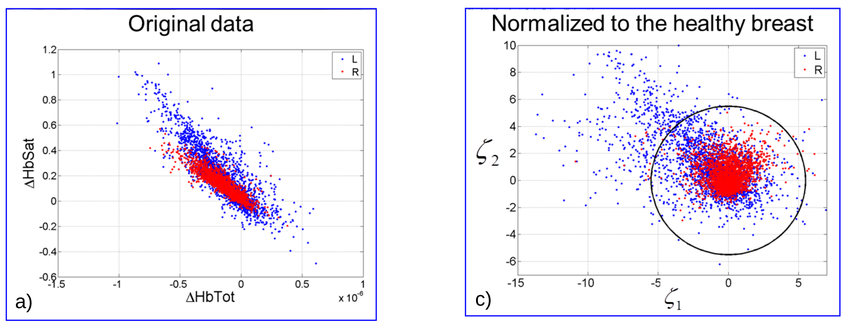

b)
$$\zeta_k^{Healthy}=\sqrt{\left(x_k^{Healthy}-\bar{x}_k^{Healthy}\right)\left(\mathbf{C}_k^{Healthy}\right)^{-1}\left(x_k^{Healthy}-\bar{x}_k^{Healthy}\right)^T},$$

$$\zeta_k^{Cancer}=\sqrt{\left(x_k^{Cancer}-\bar{x}_k^{Healthy}\right)\left(\mathbf{C}_k^{Healthy}\right)^{-1}\left(x_k^{Cancer}-\bar{x}_k^{Healthy}\right)^T},$$

Figure 4. (a) Different degrees of spreading of image values (each colored dot re[presents one image voxel) indicates that the effect of applied pressure is different in the tumor-bearing (blue dots) and healthy (red) breasts. Strong correlation between HbSat and HbTot further suggests the utility of considering this pair (among others) of hemodynamic states simultaneously. (b) A scaled value called the Mahalanobis distance (MD) [6] is a measure of extremeness for the image values in each voxel. By introducing the novel element of referencing the data for one breast to the mean and covariance for the other, the different applied-force responses are preserved in the result (c), whereas a conventional MD computation would tend to suppress them. For subsequent analysis of breast-cancer diagnosis potential, the MDs were computed by referencing each breast to the other. In this way, we avoid the use of any prior knowledge regarding the presence or absence of breast cancer, or of which was the affected breast.

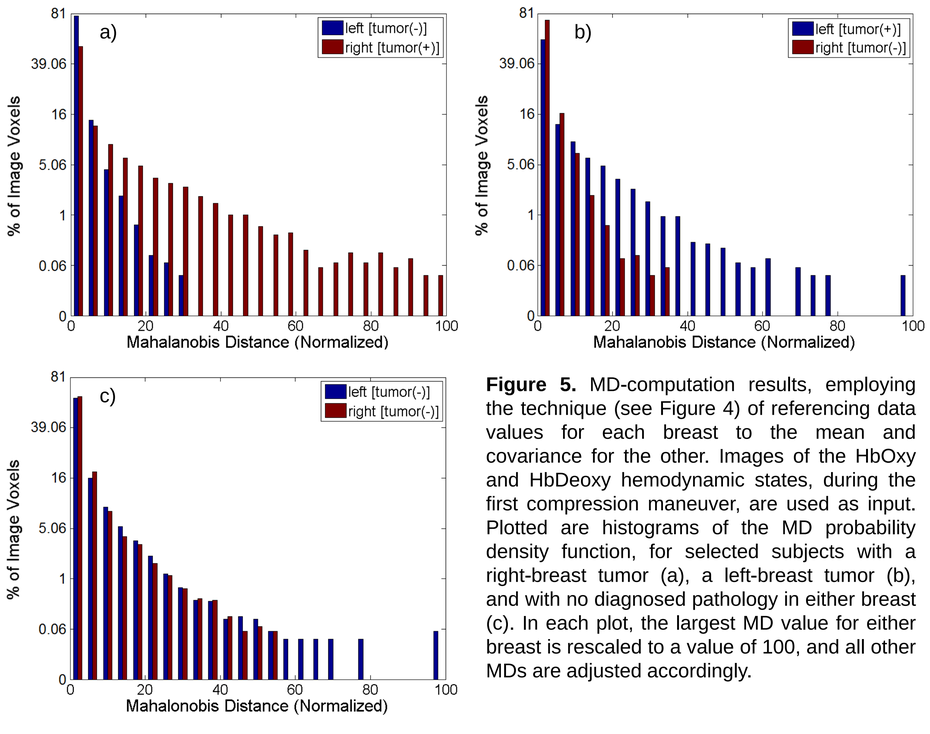

Figure 5. MD-computation results, employing the technique (see Figure 4) of referencing data values for each breast to the mean and covariance for the other. Images of the HbOxy and HbDeoxy hemodynamic states, during the first compression maneuver, are used as input. Plotted are histograms of the MD probability density function, for selected subjects with a right-breast tumor (a), a left-breast tumor (b), and with no diagnosed pathology in either breast (c). In each plot, the largest MD value for either breast is rescaled to a value of 100, and all other MDs are adjusted accordingly.

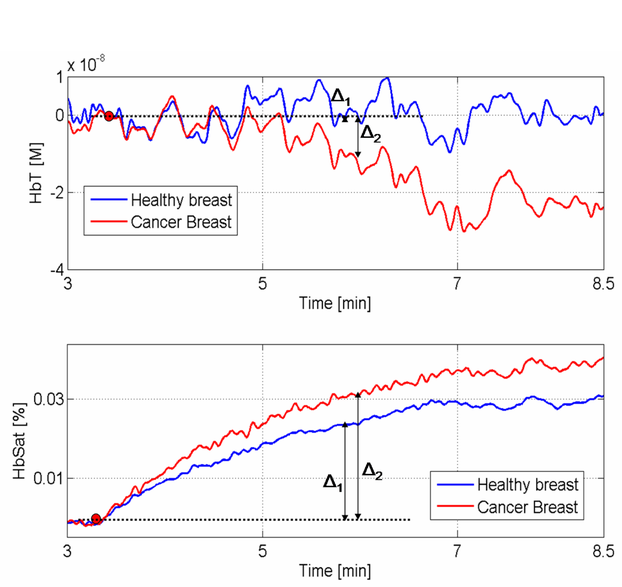

Figure 6. Representative HbTot-vs.-time (top) and HbSat-vs.-time (bottom) trends obtained during an fNIRS recording session, for a study participant with a tumor in one breast. The time interval depicted is the period immediately following the start of carbogen inspiration (large red dot), before the start of the second set of pressure maneuvers. The different responses of the two breasts indicates that carbogen inspiration can have a cancer-specific contrast-enhancing effect.

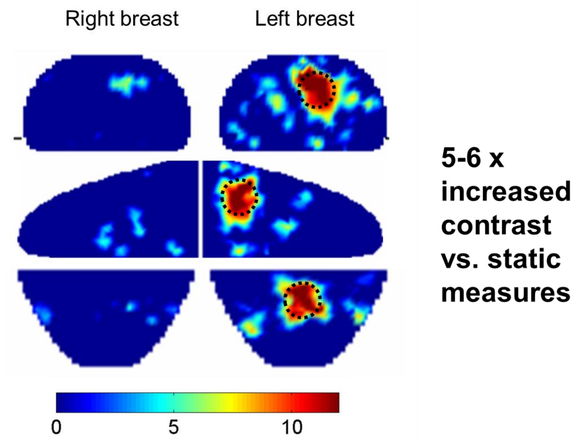

5-6 x increased contrast vs. static measures

50 y/o, BMI 44, 4 cm IDC in the left breast
MD of (ΔHbTot,ΔHbDeoxy)

Figure 7. Illustration of tumor image-contrast enhancement, resulting from use of the cross-referenced MD computation applied to force-relaxation data (see Figures 4,5). Empirically, we find that ~1% of image voxels have MD values >5 for a healthy breast. Accordingly, the images plotted here are thresholded to show only MD values ≥ 5. Dotted circles indicate the position and size of the tumor as determined from structural imaging data.

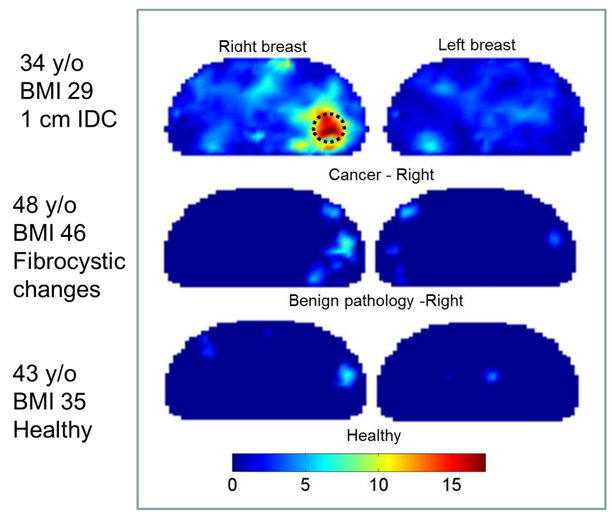

Figure 8. Illustration of tumor image-contrast enhancement, resulting from use of the cross-referenced MD computation applied to carbogen-inspiration (see Figures 4,6). Plotted images are thresholded in the same manner as in Figure 7. Dotted circle in the upper left panel indicates the position and size of the tumor as determined from structural imaging data. Corresponding results for selected subjects having either a benign breast pathology (middle row) or no diagnosed pathology (bottom row) suggest that the image-enhancing effect is specific for breast cancer.

Discussion:

- A wide range of differential responses, many of which serve to discriminate healthy from cancerous breasts, can be derived from hemodynamic responses during mechanical provocations (Fig. 5), or from adjusting the composition of the respiratory gas (Fig. 6), or from both types of maneuver performed in concert (Fig. 2).
- However, the large number of maneuvers employed (different pressure levels, full vs. partial compression, gas composition during the pressure application) gives rise to a large, multi-dimensional data mining problem. Initial tests for breast-cancer diagnostic power, considering all study participants, typically yield sensitivity and specificity values of ~75% and ~80%, respectively.
- Future efforts will focus on the choice of measurement time interval (Fig. 3) and on the choice of breast-difference metric derived from the modified MD computations (Fig. 5), as ways of improving the diagnostic sensitivity and specificity.

References:

[1] P. Vaupel, "Tumor Blood Flow," Chap. 4 in *Blood Perfusion and Microenvironment of Human Tumors: Implications for Clinical Radiooncology* (Springer, 2000), 41-45.
[2] R. Al abdi et al., "Optomechanical Imaging: Biomechanic and Hemodynamic Responses of the Breast to Controlled Articulation." http://otg.downstate.edu/Publication/AlabdiOSA12Bpost.pdf
[3] R. Al abdi, H.L. Graber, and R.L. Barbour, "Carbogen Inspiration Enhances Hemodynamic Contrast in the Cancerous Breast." http://otg.downstate.edu/Publication/AlabdiOSA12Cpost.pdf
[4] R. Al abdi, H.L. Graber, Y. Xu, and R.L. Barbour, "Optomechanical imaging system for breast cancer detection," *J. Opt. Soc. Am. A* **28**, 2473-2493 (2011).
[5] Y. Pei, H.L. Graber, and R.L. Barbour, "Influence of systematic errors in reference states on image quality and on stability of derived information for DC optical imaging," *Applied Optics* **40**, 5755-5769 (2001).
[6] R. De Maesschalck, D. Jouan-Rimbaud, and D.L. Massart, "The Mahalanobis distance," *Chemometr. Intell. Lab*. **50**, 1-18 (2000).

Acknowledgements:

This research was supported by the National Institutes of Health (NIH) grant R41CA096102, the U.S. Army grant DAMD017-03-C-0018, the Susan G. Komen Foundation, the New York State Department of Health (Empire Clinical Research Investigator Program), the New York State Foundation for Science, Technology and Innovation–Technology Transfer Incentive Program (NYSTAR-TIPP) grant C020041, and NIRx Medical Technologies.